JOC The Journal of Organic Chemistry

Article

pubs.acs.org/joc

Selective Secondary Face Modification of Cyclodextrins by Mechanosynthesis

Stéphane Menuel,[†] Bertrand Doumert,[‡] Sébastien Saitzek,[†] Anne Ponchel,[†] Laurent Delevoye,[§] Eric Monflier,[†] and Frédéric Hapiot*[,†]

[†]Unité de Catalyse et de Chimie du Solide - UCCS, CNRS UMR 8181, Université d'Artois, Faculté des Sciences Jean Perrin, SP18, 62307 Lens Cedex, France

[‡]Fédération M.E. Chevreul, CNRS FR2638, Université de Lille, Cité Scientifique, Bâtiment C4 - BP 90108, 59652 Villeneuve d'Ascq Cedex, France

[§]Unité de Catalyse et de Chimie du Solide - UCCS, CNRS UMR 8181, Ecole Nationale Supérieure de Chimie de Lille, Université de Lille, Cité Scientifique, Bâtiment C7 - BP 90108, 59652 Villeneuve d'Ascq Cedex, France

Supporting Information

ABSTRACT: α-, β-, and γ-cyclodextrins (CDs) were modified on their secondary face by mechanosynthesis at room temperature using a laboratory-scale ball-mill. Mono-2-tosylated α-, β-, and γ-CDs were obtained in good yield from mixtures of native α-, β-, and γ-CDs, respectively, *N*-tosylimidazole, and an inorganic base, with each of them being in the solid state. The yields appeared to be dependent upon the nature of the base and the reaction time. A kinetic monitoring by ^{1}H NMR spectroscopy demonstrated that the highest yields in mono-2-tosyl-CDs were measured using KOH as a base in very short reaction times (up to 65% in 80 s). Mono-(2,3-manno-epoxide) α-, β-, and γ-CDs were subsequently synthesized by ball-milling a mixture of monotosylated α-, β-, and γ-CDs, respectively, and KOH. The characterization of the modified CDs was carried out by X-ray diffraction, mass spectrometry, solid-state NMR, and diffuse reflectance UV−vis (DR UV−vis) spectroscopies. Clues to the supramolecular arrangement of the molecules in the solid state provide information on the reaction mechanism.

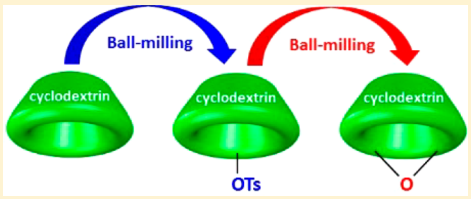

INTRODUCTION

During the past 40 years, countless publications relating to cyclodextrins (CDs) and their applications have contributed to the academic and industrial development of supramolecular chemistry.[1] CDs are torus-like macrorings built up from α-D-glucopyranose units linked together by α-1,4 glycosidic bonds (Scheme 1). The ability of native (unmodified) CDs to include molecular guests within their cavity has been widely exploited in many different fields such as drug formulations,[2,3] polymer properties control,[4,5] rotaxanes[6] and hydrogels preparation,[7,8] photochemistry,[9] and metal−organic framework.[10] However, the range of organic substrates capable of being supramolecularly recognized by the cavity of native CDs is limited. To enrich the number of CDs as molecular hosts, synthetic procedures to chemically modify their structure have been developed. Many functional groups or substituents have been covalently grafted onto the CD primary and/or secondary face, and the scope of applications has then been broadened to an impressive extent. For example, substituted CDs found application in catalysis,[11−16] enzyme mimics,[17,18] and materials[19,20] or drug delivery systems,[21,22] to name only a few possible uses.

While random substitution is relatively easy to perform, selective modification of the CD structure is a much more delicate task. Extensive efforts have been made to selectively substitute the CD primary and/or secondary faces.[23−29] However, most of the synthetic procedures implemented for these modifications required the use of organic solvents, tedious workups, and time-consuming purifications.[21,22] Accordingly, the utilization of substituted CDs on a large scale is hardly conceivable, thus hampering their industrial development. To translate scientific innovations into productive and cost-effective technology, novel chemical processes should be developed so that modified CDs are accessible in large quantities.

Recently, mechanochemistry[30] appeared as an eco-friendly alternative to access inorganic,[31−34] organic,[35−44] or metal−organic compounds[45,46] and even supramolecular host[47] and complexes[48] showing different properties to those prepared by conventional routes. For example, anti-inflammatory CD/drug composites with much higher dissolution rates were mechanochemically prepared by high-energy milling.[49] Mechanosynthesis is related to chemical reactions induced by mechanical energy. The mechanical constraints greatly enhanced the reaction selectivity, thus limiting the number of purification steps. Mechanosynthesis is usually carried out using ball-mills that grind and homogenize powders quickly and efficiently by impact and friction. Concurrently to mechanochemical milling derivatization of saccharides,[50,51] the technique has already been successfully applied to native CDs or their derivatives to favor complexation of organic molecules[52] or organic reactions in the

Received: March 30, 2015
Published: May 22, 2015

DOI: 10.1021/acs.joc.5b00697
J. Org. Chem. 2015, 80, 6259−6266

Scheme 1. Synthesis of Mono-2-tosyl CDs (*α*, 1; *β*, 2; *γ*, 3) and Mono-(2,3-manno-epoxide) CDs (*α*, 4; *β*, 5; *γ*, 6); TsIm, *N*-Tosylimidazole

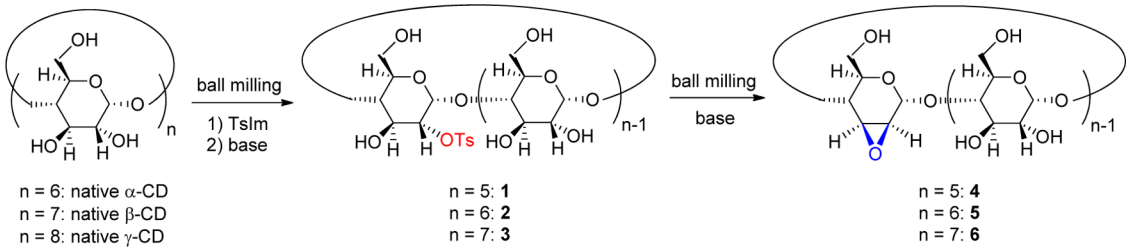

solid state within the CD cavities.[53,54] However, nothing has been described so far on the mechanosynthesis of modified CDs. In this context, we envisaged mechanosynthesis as a tool to modify the secondary face of CDs. We focused our efforts on mono-2-tosyl-CDs (*α*, **1**; *β*, **2**; *γ*, **3**) and mono-(2,3-manno-epoxide)-CDs (*α*, **4**; *β*, **5**; *γ*, **6**) (Scheme 1), which are common precursors to functionalize the CD secondary face.[23] Although the synthesis of mono-6-tosyl CDs has been widely optimized throughout the past 30 years,[55−57] tosylation on the 2-OH remains very tricky and low yields are mainly obtained.[58−66] Herein we clearly demonstrate that mechanosynthesis is a valuable tool to access these compounds in good yields in a very short reaction time. We especially describe the solvent-free synthetic procedure and characterization of the obtained products. With the support of X-ray diffraction, mass spectrometry, solid-state NMR (SSNMR), and DR UV−vis spectroscopy, a mechanism is also proposed to explain the high selectivity of tosylation at the C-2 position. Additionally, we also demonstrate that the mono-(2,3-manno-epoxide)-CDs **4**, **5**, and **6** are readily accessible from **1**, **2**, and **3** by mechanosynthesis in good yields very rapidly.

RESULTS AND DISCUSSION

Synthesis of Mono-2-tosyl-CDs. To tackle the very challenging selective 2-OH monotosylation, we used a laboratory-scale ball-mill (Retsch MM400) equipped with 10 mL zirconia grinding jars containing a zirconia ball (9 mm ⌀). The grinding jars performed radial oscillations in a horizontal position. Native CDs and *N*-tosylimidazole (TsIm) in the solid state (stoichiometric proportions) were poured in the grinding jars, which were subsequently shaken at room temperature at a 30 Hz ball-milling frequency (frequency of the rocking back-and-forth motion conducted by the reaction jar holder). Samples were regularly collected, dissolved in DMSO-d_6, and analyzed by ^{1}H NMR to determine (by comparison with reference spectra) the conversion and selectivity. Considering *α*-CD as starting material, no reaction took place even after 1.5 h without any base, whatever the frequency. Similarly, no product could be obtained using 1 equiv of $NaHCO_3$ or Li_2CO_3 as a base. Conversely, other carbonates (Na_2CO_3, K_2CO_3, Rb_2CO_3, and Cs_2CO_3) proved to be effective to activate the C-2 position. As shown in Figure 1, conversions of TsIm depended not only on the nature of the base but also on the reaction time.

Optimal conversions were almost reached within 6 min. Longer reaction times did not significantly improve the conversions. From sodium carbonate to rubidium carbonate, there seemed to be a correlation between both the water solubility and the size of the base counterion and the ability of the base to rapidly activate the 2-OH group of *α*-CD (see the Supporting Information, Figure S34). In this context, the size of

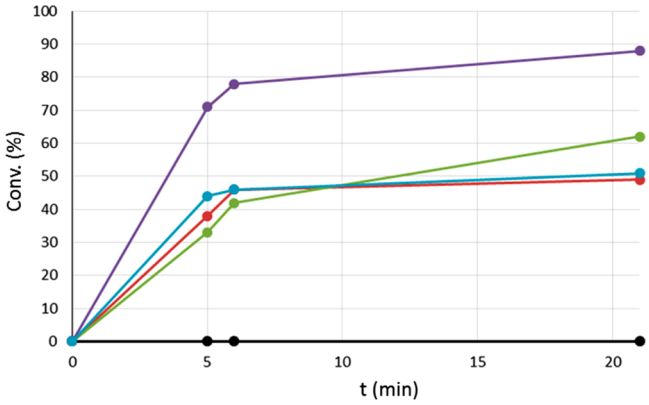

Figure 1. Conversion of TsIm with time using Li_2CO_3 (black), Na_2CO_3 (red), K_2CO_3 (green), Rb_2CO_3 (dark blue), and Cs_2CO_3 (light blue) for the synthesis of **2**.

the most water-soluble Rb_2CO_3 appeared to be the most appropriate to react with the 2-OH function. Although the reaction proceeded in the solid state, it is known that the CDs contain residual water molecules (especially outside the hydrophobic cavity). Their presence might favor both the diffusion of the base through the aqueous interstitial channels of the CD solid network and the subsequent activation of the C-2 hydroxyl group. Note that the larger size of cesium could explain the lower conversion measured using Cs_2CO_3 as a base (see Supporting Information, Figure S30). Other insights will be given later to substantiate the effect of the base on the 2-OH activation. Interesting results were also observed using hydroxyl bases. LiOH, NaOH, and KOH gave similar results, whatever their water content. Indeed, an experiment realized with dried KOH led to the same conversion and selectivity. Hydroxyl bases all proved to be faster than carbonates to activate the C-2 position. Indeed, a rapid conversion of native *α*-CD and TsIm (more than 90% conversion within 1 min) into **1** was observed (Figure 2). Nowhere in the literature does one find such a rapid process to convert native CDs into CDs functionalized on their secondary face. However, performing the reaction over a longer period of time (>15 min) strongly affected the yield of **1**, which was slowly converted into mono-(2,3-manno-epoxide)-CDs. Small quantities of polytosylated side-products were also detected by mass spectrometry (see Supporting Information, Figure S39).

The CD hydration rate was also varied to assess its impact on the tosylation reaction. Experiments were carried out with anhydrous *β*-CD (prepared by azeotropic distillation with toluene), and the results were compared to those obtained with *β*-CD containing 10% wt water. No difference was observed in terms of conversion nor selectivity.

DOI: 10.1021/acs.joc.5b00697
J. Org. Chem. 2015, 80, 6259−6266

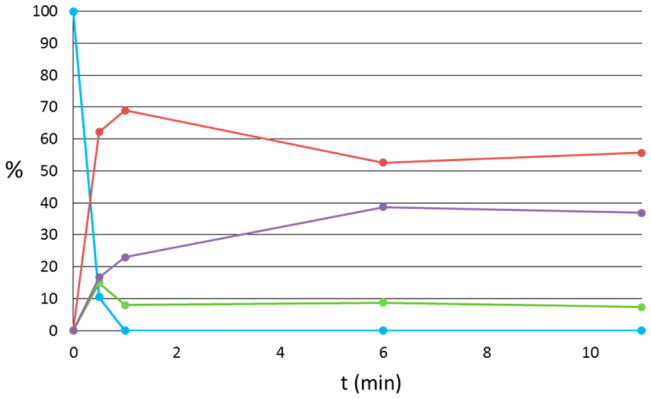

Figure 2. Variation of the proportions of TsIm and products with time at room temperature and 30 Hz frequency using α-CD as a starting material and KOH as a base. TsIm (light blue), **1** (red), *p*-toluenesulfonic acid (dark blue), and polytosylated side-products (green).

We then sought to optimize the syntheses by varying the ball-milling frequency and the reaction time using two different methods. In the first approach (method A), the CD and TsIm were ball-milled in stoichiometric proportions for 2 min and KOH (1 equiv) was added afterward. In a second approach (method B), the CD and KOH were first mixed together in stoichiometric proportions and TsIm (1 equiv) was subsequently added. Whatever the method (A or B), the mixtures were shaken at 15, 25, or 30 Hz. From the TsIm conversion, kinetic profiles were drawn at three different frequencies as a function of the reaction time (Figure 3).

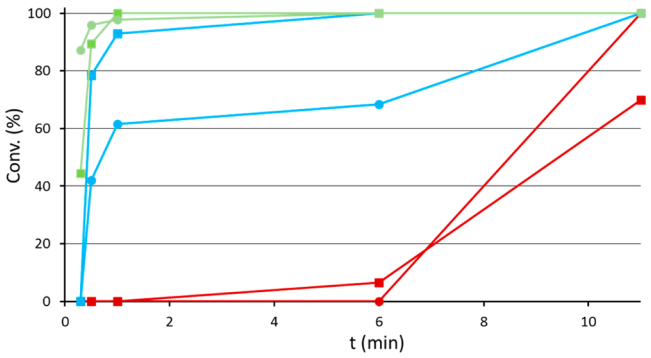

Figure 3. TsIm conversion with time for α-CD as starting material and KOH as a base using method A at 15 Hz (red square), method A at 25 Hz (light blue square), method A at 30 Hz (green square), method B at 15 Hz (red circle), method B at 25 Hz (light blue circle), and method B at 30 Hz (green circle).

Apart from the experiments realized at 25 Hz for which the same conversion was observed within 11 min following a different profile, no significant difference was noticed between method A and method B in terms of reactivity. The best results were obtained at 30 Hz, suggesting that higher frequencies led to an increase in both the temperature and the surface area with beneficial effects on the chemical activity of the powders. In that case, 100% and 98% TsIm were converted within 1 min using method A and method B, respectively. However, method A was more selective than method B as higher proportions of **1** were formed using method A (69% vs 59% for method B). Accordingly, the order of addition of the reactants is not inconsequential. Mixing first the CD and the base (method B) favored the formation of polytosylated CDs upon addition of TsIm, thus affecting the yield of **1**. In terms of purity and yields, the current approach was far more effective than synthetic procedures from the literature for which a preliminary protection of the CD primary face was often required and low yields of products were isolated.[58,67,68]

The scaling-up of the process was carried out using 50 mL stainless steel grinding jars containing one steel ball (25 mm ⌀, 63.2 g) using method A. Within 2 min, 100% TsIm were converted. Although already high compared to literature data, the conversions could probably be further optimized by a judicious choice of the ball-milling apparatus, especially for large quantities of reactants.

Characterization. To get more information on the selectivity of the tosylation reaction in the 2-position, reactants and products were analyzed through ^{13}C CP/MAS solid-state NMR experiments. As previously reported by Pessine et al.,[69] ^{13}C chemical shifts of molecular guests were affected by several ppm as an evidence of encapsulation into the CD cavity. The ^{13}C NMR spectrum of a 1/1 mixture of native β-CD and TsIm was compared to those of the separated components (see Supporting Information, Figure S29).

No chemical shift change of the ^{13}C signals assigned to the CD (region 59−105 ppm) was evidenced. No amorphization occurred during mechanosynthesis as revealed by the similar ^{13}C line widths measured for native CD and in the mixture. However, a clear variation of the chemical shift was observed for those aromatic protons of the TsIm in the mixture (compare Figures 4a and 4b), suggesting an interaction between the native β-CD and tosylimidazole.

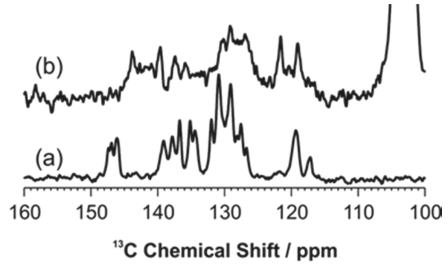

Figure 4. ^{13}C CP/MAS NMR spectra of (a) TsIm and (b) a 1/1 mixture (1.3 mmol each) of native β-CD and TsIm at 25 °C.

As a complement to ^{13}C CP/MAS NMR and in order to probe the spatial proximity of TsIm and β-CD, we resorted to ^{1}H−^{1}H double-quantum/single-quantum (DQ-SQ) spectroscopy. It must be emphasized that DQ-SQ makes use of the homonuclear dipole−dipole coupling to yield correlations between pairs of protons in a two-dimensional (2D) fashion. In practice, cross-peaks at chemical shift $\delta_1 + \delta_2$ in the DQ dimension reflect the short distance, and thus the proximity, between protons of two types at chemical shift δ_1 and δ_2 in the SQ dimension.[70,71] The ^{1}H−^{1}H 2D spectrum of a 1/1 mixture of native β-CD and TsIm (1.3 mmol each) is presented in Figure 5. Here, the use of high-field (B_0 = 18.8 T) and ultrahigh spinning speed (MAS spinning frequency of 60 kHz) was highly beneficial in terms of resolution, as demonstrated by the ^{1}H 1D MAS NMR spectrum (top projection, Figure 5). The ^{1}H MAS NMR spectrum showed two chemical shift regions, assigned to the CD (2−7 ppm) and to TsIm (7−8 ppm). The DQ-SQ spectrum clearly revealed cross-correlation between the aromatic imidazolium protons (in the 8.5−7.5 ppm region) and the β-CD protons (in the 4.2−3.5 ppm

DOI: 10.1021/acs.joc.5b00697
J. Org. Chem. 2015, 80, 6259−6266

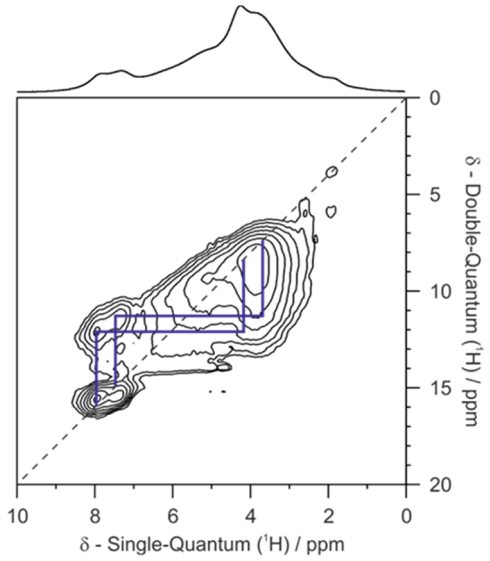

Figure 5. $^{1}H-^{1}H$ double-quantum MAS NMR spectrum of a 1/1 mixture of native β-CD and tosylimidazole (1.3 mmol each) at 25 °C.

region), indicative of the inclusion of the imidazole moiety into the CD cavity.

DR UV−visible spectroscopy was also informative on the formation of new species during the course of the reaction. When increasing amounts of TsIm were added to native CD-containing solutions, an absorption characteristic of a new electronic transition was revealed in the 270−280 nm region (see Supporting Information, Figure S35). The changes in the position and intensity of the band are assumed to results from changes in the solid microenvironment upon inclusion of TsIm into the CD cavity. The red shift in the absorbance maximum (bathochrome effect) was presumably caused by the imidazole ring being complexed in the hydrophobic interior of the CD cavity as already shown for other aromatic guests.[72] Knowing that the thermodynamic activity of pure substances in the solid phase is normally taken as unity, the stoichiometry of the CD/TsIm complexes could be determined by DR UV−vis spectroscopy through a method of continuous variation (Job's plot). As an example, the Job's plot of the α-CD/TsIm couple is given in Figure 6. Although the solid CD/TsIm mixture could not be as homogeneously distributed as in solution, the DR UV−vis data tend to support the hypothesis of a 2:1 equilibrium with a maximum shift of 0.08 at f(TsIm) 0.3, meaning that two CDs interacted with only one TsIm (Supporting Information). Increasing the size of the CD cavity (β-CD and γ-CD) also led to a 2:1 stoichiometry for the CD/TsIm complex (see Supporting Information, Figures S36 and S37).

The interaction between the CDs and imidazole was also highlighted by X-ray diffraction (XRD). Figure 7 shows the XRD patterns of β-CD and β-CD/KOH as prepared by ball-milling (30 Hz, 2 min). The XRD pattern of β-CD (Figure 7a) presents a crystalline structure similar to that described by C. Betzel et al.[73] It crystallized in monoclinic structure with $P2_1$ space group whose lattice parameters were a = 21.261(6) Å, b = 10.306(3) Å, c = 15.123(4) Å, and β = 112.3(5)°. The XRD pattern of β-CD/KOH (Figure 7b) had the same characteristic peaks as the unmixed β-CD. Only a slight amorphization resulting in a broadening of the diffraction peaks (beginning of the formation of an amorphous halo between 2θ = 16.5° and 22°) was observed. KOH is a deliquescent solid through air moisture.

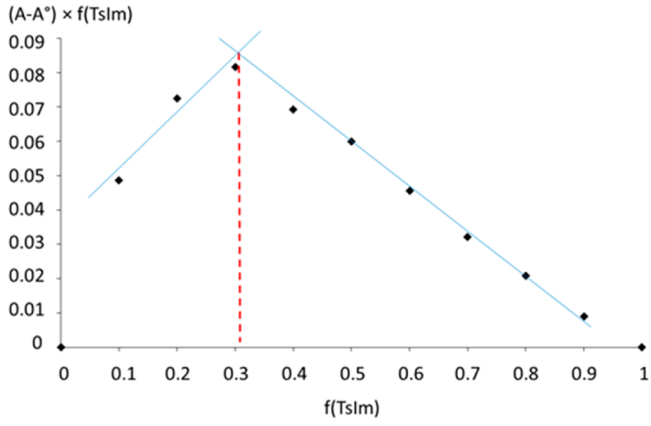

Figure 6. Continuous variation plot (Job's plot) derived from UV−vis measurements realized at 20 °C and 30 Hz for 2 min (see Supporting Information) for α-CD/TsIm mixtures. f(TsIm) = [TsIm]/([TsIm] + [α-CD]). A = absorbance of α-CD/TsIm mixtures (total amount = 2.65 mmol). A^0 = absorbance of TsIm (2.65 mmol).

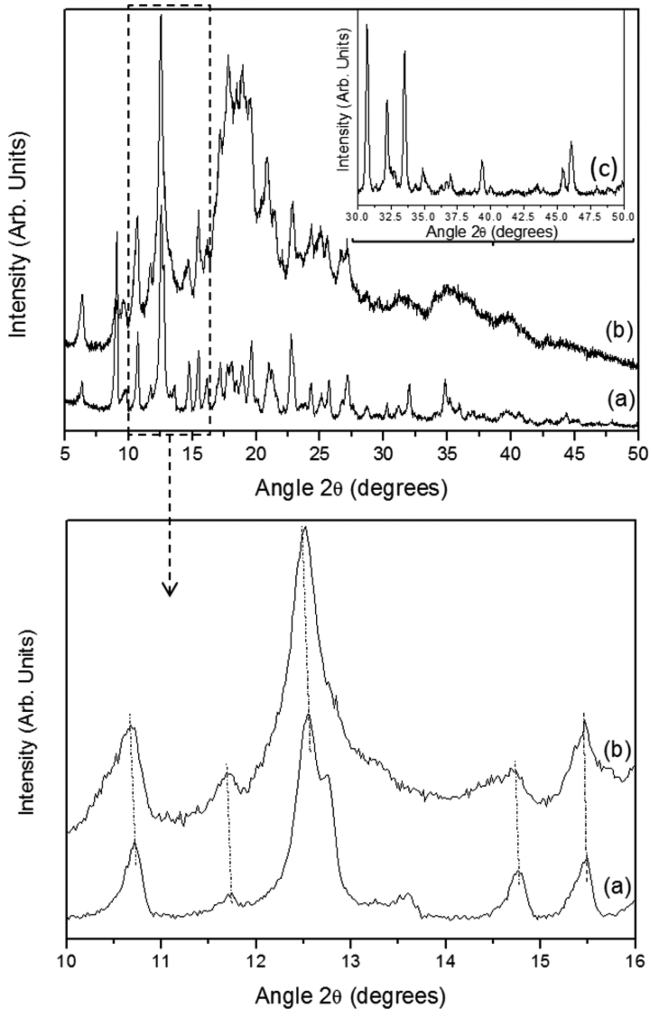

Figure 7. XRD patterns of β-CD (a), β-CD/KOH (b), and KOH (c) after mixing in a ball-mill at 30 Hz for 2 min.

Therefore, it is possible that it deteriorated, thus explaining the absence of any diffraction peak. To check whether there was a deliquescence of KOH, an XRD pattern of KOH was performed after ball-milling. The diffractogram was achieved immediately

DOI: 10.1021/acs.joc.5b00697
J. Org. Chem. 2015, 80, 6259−6266

after grinding under dry atmosphere, as for the β-CD/KOH sample. The XRD pattern (inset in Figure 7) showed that KOH crystallized in its hydrated form (KOH, H_2O) with a monoclinic structure (JCPD no. 36-791). No peak attributable to the KOH, H_2O phase was identified in the β-CD/KOH sample (Figure 7). The absence of a peak could be explained by the deliquescence of KOH resulting from the β-CD crystallization water molecules during the ball-milling process. However, this did not explain the shift of the diffraction peaks toward smaller angles values. Indeed, this shift could be explained by a slight increase in the crystallographic cell compared to the initial β-CD, probably caused by an interaction between β-CD and KOH.

Figure 8 shows the XRD patterns of β-CD, TsIm, and β-CD/TsIm compound obtained by ball-milling (30 Hz, 2 min). The

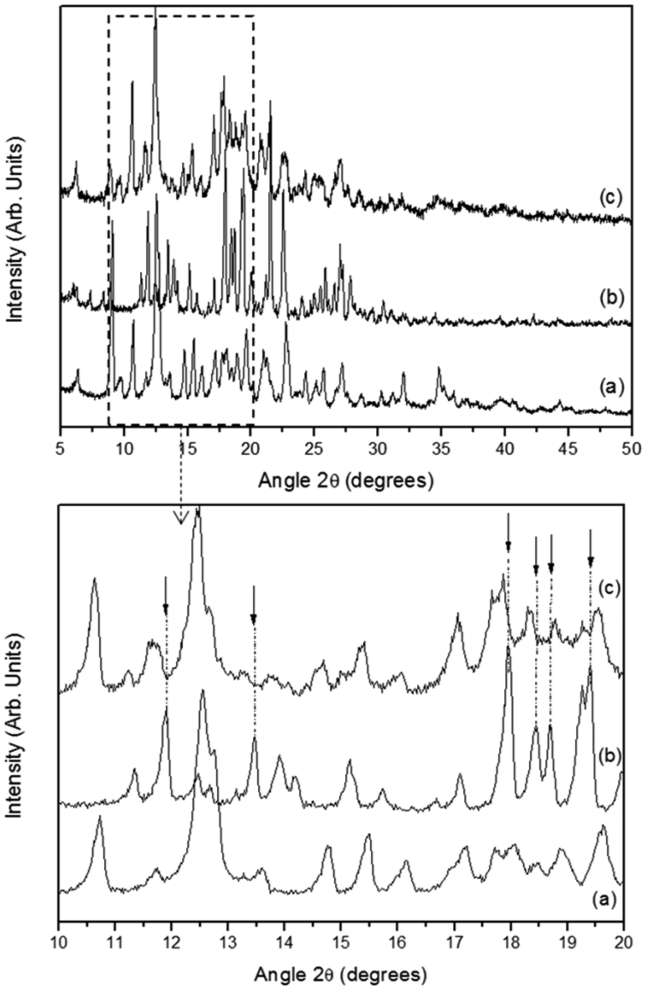

Figure 8. XRD patterns of (a) β-CD, (b) TsIm, and (c) β-CD/TsIm after mixing by high-energy ball-milling at 30 Hz for 2 min.

diffractograms of the β-CD/TsIm and the initial compounds differ markedly in their diffraction peak positions. In other words, the XRD pattern obtained for β-CD/TsIm compound was not the direct superposition of diffractograms from the starting compounds. It was no longer possible to distinguish the characteristic peaks of TsIm (arrows in Figure 8b). This behavior could be explained by the encapsulation of the "guest" molecule into the β-CD cavity or the reaction between the two precursors giving rise to a new crystallized structure.

Mechanism. Spectroscopic and diffraction data outlined above prompted us to propose a mechanism to explain the selectivity of the tosylation at the 2-position. In the first step, CD/TsIm supramolecular complexes formed rapidly by inclusion of the hydrophobic methylphenyl moiety of TsIm into the CD cavity (Scheme 2). In the second step, the 2-OH and 3-OH protons are deprotonated. Indeed, they have similar pK_A and can undergo a rapid deprotonation.[74]

However, the data clearly showed that the existence of a supramolecular CD/TsIm complex selectively oriented the tosylation reaction on the 2-OH group. Indeed, once TsIm was included into the CD cavities, only the deprotonated 2-OH groups (inwardly facing the CD cavities) could react in a third step with the tosylate functions, thus leading selectively to mono-2-*O*-tosyl CDs. The deprotonated 3-OH group, for its part, remained unchanged as it pointed outside the CD cavity. Thus, the 2-tosylation was controlled by the relative positions of the reactants in the constrained environment of the CD cavity (reaction-cavity concept).[75−77] Additionally, as recently described in the literature for CDs dissolved in aqueous solution,[78] we suggest that the replacement of high-energy water molecules in CD cavities by hydrophobic TsIm guests is the essential enthalpic driving force for complexation and diffusion of TsIm along the hydrophobic CD channels. Thus, although the experimental conditions of the ball-milling process are very far from those relative to aqueous solution, the same hydrophobic effects can be incriminated to explain the selectivity of the substitution reaction. Note that a control experiment carried out with the noncyclic methyl-α-D-glucopyranoside (**7**) (see Supporting Information) in the same reaction conditions led exclusively to a 6-tosylation, thus highlighting the role of the CD cavity toward the reaction selectivity.

Synthesis of Mono-(2,3-manno-epoxide)-CDs. The beneficial effect of mechanosynthesis on the selective modification of CDs was further demonstrated in the synthesis of other secondary face functionalized CDs, namely, mono-(2,3-manno-epoxide)-CDs **4**, **5**, and **6** (Scheme 1). These CDs are key reactants for the synthesis of various CDs substituted on their secondary face.[23] They were synthesized by mechanosynthesis from **1**, **2** and **3**, respectively, as follows: a stoichiometric mixture of mono-2-*O*-tosyl-CD and KOH was ball-milled at 30 Hz for 2 h. The resulting powder was purified by flash chromatography using a CH_3CN/H_2O mixture to give **4**, **5**, and **6** as white powders in good yields (61%, 63%, and 67%, respectively). A kinetic profile (see Supporting Information, Figure S38) showed a rapid conversion of **2** into **5** (50% of mono-2-*O*-tosyl-β-CDs was converted within only 20 min). Afterward, the conversion leveled off to reach 70%. Note that the direct syntheses of **4**, **5**, and **6** were also attempted from native CDs using 2 equiv of KOH, but the high reactivity of the hydroxyl anions toward the 2-OH groups (compared to the nucleophilic substitution rate) led to numerous deprotonations resulting in the formation of polytosylated CDs, as already commented previously for the CD 2-tosylation.

Conclusions. Although grinding has already been extensively applied to the supramolecular concepts,[79] nothing was described so far on the selective mechanosynthesis of CDs functionalized onto their secondary hydroxyl rim through supramolecular means. In this study, the synthesis of two key CD-based building blocks was performed by ball-milling. While the synthesis of mono-2-*O*-tosyl CDs and mono-(2,3-manno-epoxide) CDs is a very delicate task using the classical tools of organic chemistry, solid-state reactions allowed us to obtain rapidly and selectively large amounts of these compounds with very good purity. Moreover, we demonstrated that supramolecular chemistry is

DOI: 10.1021/acs.joc.5b00697
J. Org. Chem. 2015, 80, 6259−6266

Scheme 2. Proposed Mechanism for the Two-Step Synthesis of Mono-2-*O*-tosylated CDs by Ball-Milling

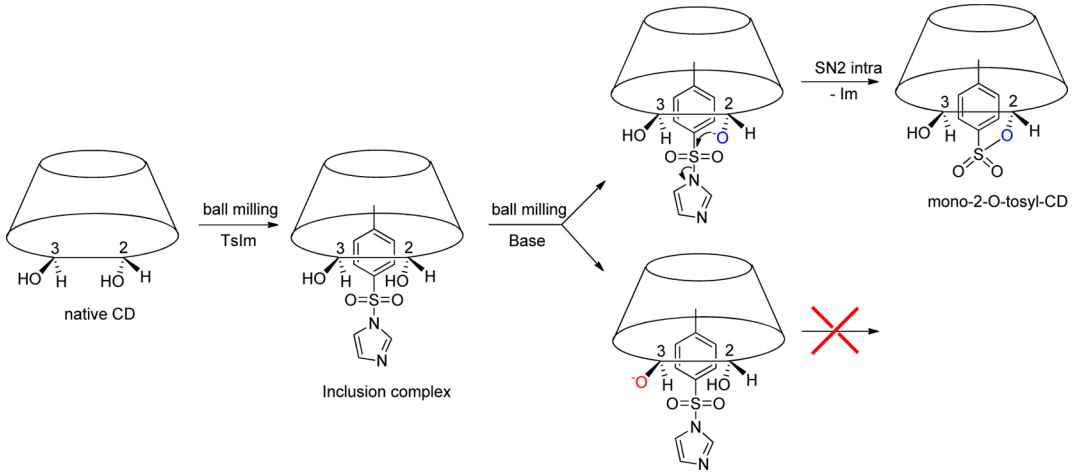

involved in the conversion of native CDs into functionalized CDs using grinding technique.

EXPERIMENTAL SECTION

Materials and Methods. All chemicals were used as received. Analytical thin-layer chromatography (TLC) was performed on aluminum-backed silica gel. Reactions were carried out using a laboratory-scale ball-mill (Retsch MM400) equipped with 10 mL zirconia grinding jars containing one zirconia ball (9 mm ⌀, 5.4 g). The frequency of the ball-mill represents the oscillation of the milling beakers. It is not related to the number of impacts, which depends on the frequency of the ball mill, the number of balls, and the filling degree. The data were collected as follows: The ball mill was stopped at a given time. A sample of the powder was collected and analyzed. The ball mill was then restarted. The procedure was repeated as often as necessary. Each reaction was repeated twice to ensure the repeatability of the results. Each data point is the average of the two obtained values. Compounds were identified using UV fluorescence and/or staining with a solution of 5% vol sulfuric acid in ethanol. NMR spectra were recorded on a spectrometer operating at 300 MHz for ^{1}H nuclei and 75 MHz for ^{13}C nuclei in $CDCl_3$ (99.50% isotopic purity), DMSO-d_6 (99.80% isotopic purity), or D_2O (99.92% isotopic purity). Solid-state NMR spectra were acquired on a spectrometer operating at 100.62 MHz for ^{13}C nuclei and a spectrometer operating at 800.13 MHz for ^{1}H nuclei. For the ^{13}C MAS spectra, a cross-polarization (CP) from the protons was used to generate the initial ^{13}C signal, followed by data acquisition under ^{1}H decoupling. Contact time (CT) RF-field amplitudes were set to 70 and 60 kHz for ^{1}H and ^{13}C, respectively, with the use of a ramp on the ^{1}H channel. The ^{1}H decoupling RF field amplitude was set to 80 kHz using a SPINAL64 decoupling scheme.[80] A total of 1024 transients was added, with a relaxation delay of 5 s between each scan, a CP contact time of 1.5 ms, at a MAS spinning speed of 10 kHz. A Lorentzian line-broadening function of 5 Hz was applied for ^{13}C CP/MAS spectra presented in ESI and of 25 Hz in Figure 4. A two-dimensional ^{1}H−^{1}H double quantum magic-angle spinning spectrum was performed at 60 kHz spinning speed using the $R12_2^5$ symmetry-based recoupling scheme applied for 110 μs at an RF field strength of 180 kHz.[81] The recycling delay was set to 1 s, and 256 transients were added for each of the 64 t_1 increments. Chemical shifts were given in ppm with respect to TMS as external reference for ^{1}H and ^{13}C NMR spectra. The UV−vis spectra of the solid samples were recorded in the diffuse reflectance mode on a spectrophotometer equipped with a 60 mm integrating sphere. The solid powders were placed in quartz sample holders while $BaSO_4$ was used as a white standard. Spectra were plotted in $F(R_\infty)$ Kubelka−Munk units with

$$F(R_\infty) = \frac{(1 - R_\infty)^2}{2R_\infty}$$

where R_∞ is the diffuse reflectance of an infinite-thickness layer. Job Plots were drawn from UV−vis measurements as follows: a series of solutions containing CD and TsIm were prepared such that the sum of their total concentration remained constant (2.65 mM). The TsIm mole fraction f(TsIm) was varied from 0.1 to 1.0. The corrected absorbance $(A - A^\circ) \times$ f(TsIm) at 280 nm was plotted against the molar fraction of the TsIm solution. Each reaction was repeated twice to ensure the repeatability of the results. Each data point is the average of the two obtained values. Mass spectra were recorded on a MALDI-TOF−TOF spectrometer in positive reflectron mode with 2,5-dihydroxybenzoic acid (2,5-DHB) as matrix. Organic compounds were characterized by X-ray diffraction (XRD). The XRD pattern was recorded on a diffractometer (in Bragg−Brentano geometry) equipped with copper X-ray source ($\lambda K_{\alpha 1}$ = 0.15406 and $\lambda K_{\alpha 2}$ = 0.15449 nm) and Soller slits. A nickel filter was used to remove the Cu Kβ radiation. The pattern was recorded for angular range (2θ) from 5° to 50° with a step of 0.04° and counting time of 10 s per step. The CD water content was calculated by gravimetric measurements. The weight difference between hydrated CD and anhydrous CD allowed for determining the CD water content. To obtain anhydrous β-CD, β-CD was dried using a Dean−Stark apparatus in boiling toluene. After removing toluene by azeotropic distillation using a rotary evaporator, anhydrous β-CD was preserved under vacuum at 120 °C overnight before use. Anhydrous KOH was prepared under vacuum at 110 °C and preserved in a vacuum desiccator over P_2O_5.

Mono-2-*O*-tosyl-α-cyclodextrin (1). A mixture of α-CD[82] (1 g, 1.03 mmol) and *p*-toluenesulfonyl imidazole[83] (229 mg, 1.03 mmol) was ball-milled for 5 min at 30 Hz in a 10 mL zirconia reactor containing one zirconia ball (9 mm ⌀). One equivalent of KOH (58 mg, 1.03 mmol) was then added to the mixture and ball-milled at 30 Hz for 80 s. The powder was collected using 5 mL of dry DMSO and filtered. One was precipitated by addition of 50 mL of acetone. Further purification by flash chromatography on silica gel using an acetonitrile/water (8:2) eluent system gave **1** as a white powder; isolated yield, 47% (545 mg). ^{1}H NMR (300 MHz, DMSO-d_6, 298 K): δ 7.86 (d, J = 8.16 Hz, 2H, H_b); 7.45 (d, J = 8.16 Hz, 2H, H_c); 5.73−5.44 (m, 11H, OH_2, OH_3); 4.79 (m, 6H, H_1); 4.52−4.43 (m, 6H, OH_6); 4.08−3.98 (m, 4H, H'_2, H'_3, H'_4); 3.84−3.45 (complex m, 25H, H_3, H_2, H_5, H_6); 3.42 (m, overlapped with H_2O); 2.42 (s, 3H, CH_3). ^{13}C{^{1}H} NMR (75 MHz, D_2O, 298 K): δ 145.5 (C_a); 133.1 (C_d); 130.4 (C_c); 128.6 (C_b); 102.8 (C_1); 99.1 (C'_1); 82.4 (C_4); 79.9 (C'_2); 73.7−72.6−72.0 (C_3, C_2, C_5); 69.6 (C'_3); 60.4 (C_6); 21.6 (CH_3). MS: m/z calcd for $[C_{43}H_{66}O_{32}S + H]^+$ 1127.33, obsd 1130.99; calcd for $[C_{43}H_{66}O_{32}S + Na]^+$ 1149.32, obsd 1149.11; calcd for $[C_{43}H_{66}O_{32}S + K]^+$ 1165.29, obsd 1165.10. Anal. Calcd for $C_{43}H_{66}O_{32}S \cdot 2H_2O$: C, 44.41; H, 6.07; O, 46.77; S, 2.76. Found: C, 44.48; H, 5.99; O, 46.84; S, 2.83.

Mono-2-*O*-tosyl-β-cyclodextrin (2). Compound **2** was prepared according to the procedure used for the synthesis of **1** by reacting β-CD[82] (1 g, 0.88 mmol), *p*-toluenesulfonyl imidazole (195 mg, 0.88 mmol), and KOH (49 mg, 0.88 mmol); isolated yield, 53% (589 mg).

DOI: 10.1021/acs.joc.5b00697
J. Org. Chem. 2015, 80, 6259−6266

^{1}HNMR (300 MHz, DMSO-d_6, 298 K): δ 7.95 (d, J = 8.40 Hz, 2H, H_b); 7.54 (d, J = 8.40 Hz, 2H, H_c); 6.10−5.75 (m, 13H, OH_2, OH_3); 4.93 (m, 7H, H_1); 4.57 (m, 7H, OH_6); 4.34 (d, J = 3.9 Hz, 1H); 4.04 (m, 1H); 3.70 (m, 1H); 3.74−3.60 (complex m, 30H, H_3, H_2, H_5, H_6); 3.47 (m, overlapped with H_2O); 2.52 (s overlapped with DMSO, CH_3). $^{13}C\{^1H\}$ NMR (75 MHz, D_2O, 298 K): δ 145.0 (C_a); 132.9 (C_d); 129.9 (C_c); 128.1 (C_b); 101.9 (C_1); 101.8 (C'_1); 81.5 (C_4); 80.9 (C'_2); 73.0−72.3−72.1 (C_3, C_2, C_5); 69.3 (C'_3); 59.9 (C_6); 21.2 (CH_3). MS: m/z calcd for $[C_{49}H_{76}O_{37}S + Na]^+$ 1311.37, obsd 1310.92; calcd for $[C_{49}H_{76}O_{37}S + K]^+$ 1327.34, obsd 1326.90. Anal. Calcd for $C_{49}H_{76}O_{37}S{\cdot}3H_2O$: C, 43.82; H, 6.15; O, 47.64; S, 2.39. Found: C, 43.75; H, 6.25; O, 47.65; S, 2.35.

Mono-2-*O*-tosyl-γ-cyclodextrin (3). Compound **3** was prepared according to the procedure used for the synthesis of **1** by reacting γ-CD[82] (1 g, 0.77 mmol), *p*-toluenesulfonyl imidazole (171 mg, 0.77 mmol), and KOH (43 mg, 0.77 mmol); isolated yield, 21% (234 mg). ^{1}HNMR (300 MHz, DMSO-d_6, 298 K): δ 7.85 (d, J = 8.25 Hz, 2H, H_b); 7.44 (d, J = 8.25 Hz, 2H, H_c); 5.70 (m, 15H, OH_2, OH_3); 5.18 (d, J = 3.33 Hz, 1H, H'_1); 4.88 (m, 7H, H1); 4.64−4.52 (m, 7H, OH_6); 4.39 (d, J = 4.4 Hz, OH_6′1H); 4.08 (dd, J = 3.3 Hz, J = 10 Hz, 1H); 3.87 (m, 2H); 3.65−3.48 (complex m, 31H, H_3, H_2, H_5, H_6); 3.40 (m, overlapped with H_2O); 2.41 (s, 3H, CH_3). $^{13}C\{^1H\}$ NMR (75 MHz, D_2O, 298 K): δ 145.2 (C_a); 133.7 (C_d); 130.3 (C_c); 128.6 (C_b); 102.0 (C_1); 97.6 (C'_1); 80.9 (C_4); 78.4 (C'_2); 73.5−73.2−72.6 (C_3, C_2, C_5); 69.5 (C'_3); 60.3 (C_6); 21.7 (CH_3). MS: m/z calcd for $[C_{55}H_{86}O_{42}S + Na]^+$ 1473.42, obsd 1473.12; calcd for $[C_{55}H_{86}O_{42}S + K]^+$ 1489.40, obsd 1489.10. Anal. Calcd for $C_{55}H_{86}O_{42}S{\cdot}6H_2O$: C, 42.36; H, 6.33; O, 49.25; S, 2.06. Found: C, 42.44; H, 6.31; O, 49.27; S, 2.09.

Mono-(2,3-manno-epoxide) α-CD (4). A stoichiometric mixture of **1** (780 mg, 0.69 mmol) and KOH (39 mg, 0.49 mmol) was ball-milled at 30 Hz for 2 h. The resulting powder was chromatographed on silica gel using an acetonitrile/water (8:2) eluent system. **4** was isolated as a white powder. Isolated yield: 61% (401 mg). ^{1}H NMR (300 MHz, D_2O, 298 K): δ 5.24 (s, 1H, H_{1m}); 5.01 (complex m, 5H, H_1); 3.98−3.78 (complex m, 21H, H_3, H_6, H_{4m}, H_5); 3.72−3.50 (m, 14H, H_{6m}, H_{3m}, H_{5m}, H_2, H_4); 3.44 (d, 1H, J = 3.3 Hz, H_{2m}). $^{13}C\{^1H\}$ NMR (75 MHz, D_2O, 298 K): δ 101.1−100.8 (C_1); 97.3 (C_{1m}); 80.8 (C_4); 72.8−72.3−71.6 (C_2, C_3, C_5); 70.3 (C_{4m}); 69.9 (C_{5m}); 61.1 (C_{6m}); 60.1 (C_6); 52.9 (C_{3m}); 48.4 (C_{2m}). MS: m/z calcd for $[C_{36}H_{58}O_{29} + Na]^+$ 977.30, obsd 977.29; calcd for $[C_{36}H_{58}O_{29} + K]^+$ 993.27, obsd 993.29. Anal. Calcd for $C_{36}H_{58}O_{29}{\cdot}2H_2O$: C, 43.64; H, 6.31; O, 50.05. Found: C, 43.58; H, 6.37; O, 50.15.

Mono-(2,3-manno-epoxide) β-CD (5). Compound **5** was prepared according to the procedure used for the synthesis of **4** by reacting **2** (636 mg, 0.49 mmol) and KOH (28 mg, 0.49 mmol); isolated yield, 63% (344 mg). ^{1}H NMR (300 MHz, D_2O, 298 K): δ 5.25 (s, 1H, H_{1m}); 5.07 (complex m, 6H, H_1); 3.98−3.79 (complex m, 25H, H_3, H_6, H_{4m}, H_5); 3.72−3.46 (m, 16H, H_{6m}, H_{3m}, H_{5m}, H_2, H_4); 3.46 (d, 1H, J = 3.8 Hz, H_{2m}). $^{13}C\{^1H\}$ NMR (75 MHz, D_2O, 298 K): δ 101.5 (C_1); 97.9 (C_{1m}); 80.7 (C_4); 72.8−71.8−71.6 (C_2, C_3, C_5); 70.3 (C_{4m}); 69.6 (C_{5m}); 61.0 (C_{6m}); 60.3 (C_6); 54.1 (C_{3m}); 49.2 (C_{2m}). MS: m/z calcd for $[C_{42}H_{68}O_{34} + Na]^+$ 1139.35, obsd 1139.38; calcd for $[C_{42}H_{68}O_{34} + K]^+$ 1155.32, obsd 1155.36. Anal. Calcd for $C_{42}H_{68}O_{34}{\cdot}2H_2O$: C, 43.75; H, 6.29; O, 49.95. Found: C, 43.82; H, 6.30; O, 49.87.

Mono-(2,3-manno-epoxide) γ-CD (6). Compound **6** was prepared according to the procedure used for the synthesis of **4** by reacting **3** (450 mg, 0.31 mmol) and KOH (17 mg, 0.49 mmol); isolated yield, 67% (265 mg). ^{1}H NMR (300 MHz, D_2O, 298 K): δ 5.25 (s, 1H, H_{1m}); 5.11 (complex m, 7H, H_1); 3.95−3.73 (complex m, 29H, H_3, H_6, H_{4m}, H_5); 3.70−3.50 (m, 17H, H_{6m}, H_{3m}, H_{5m}, H_2, H_4); 3.45 (d, 1H, J = 3.6 Hz, H_{2m}). $^{13}C\{^1H\}$ NMR (75 MHz, D_2O, 298 K): δ 101.3 (C_1); 97.1 (C_{1m}); 80.1 (C_4); 71.8−72.1−71.6 (C_2, C_3, C_5); 69.2 (C_{4m}, C_{5m}); 60.8 (C_{6m}); 60.2 (C_6); 54.3 (C_{3m}); 49.5 (C_{2m}). MS: m/z calcd for $[C_{48}H_{78}O_{39} + Na]^+$ 1301.40, obsd 1301.41; calcd for $[C_{48}H_{78}O_{39} + K]^+$ 1317.38, obsd 1317.41. Anal. Calcd for $C_{48}H_{78}O_{39}{\cdot}4H_2O$: C, 42.67; H, 6.42; O, 50.92. Found: C, 42.69; H, 6.49; O, 50.98.

Methyl-6-*O*-tosyl-α-D-glucopyranoside (7). Methyl-α-D-glucopyranoside (1500 mg, 7.72 mmol) and *p*-toluenesulfonyl imidazole (245 mg, 1.10 mmol) were ball-milled for 5 min at 30 Hz in a 10 mL zirconia reactor containing one zirconia ball (9 mm in diameter). KOH (62 mg, 1.10 mmol) with regard to methyl-α-D-glucopyranoside was then added, and the mixture was ball-milled at 30 Hz for 5 min. The powder was further dissolved in 5 mL of dry DMSO. After filtration, the monotosylated methyl-6-*O*-tosyl-α-D-glucopyranoside (**7**) was precipitated by addition of 100 mL of chloroform. The product was further purified by flash chromatography on silica gel using an acetonitrile/water (8/2, v/v) mobile phase. Isolated yield: 9% (240 mg). ^{1}H NMR (300 MHz, DMSO-d_6, 298 K): δ 7.76 (d, 2H, J = 8.39 Hz, H_b); 7.49 (d, 2H, J = 8.39 Hz, H_a); 5.17 (d, 1H, J = 5.89 Hz, OH_4); 4.89 (d, 1H, J = 5.18 Hz, OH_3); 4.82 (d, 1H, J = 6.42 Hz, OH_2); 4.48 (d, 1H, J = 4.27 Hz, H_1); 4.21 (dd, 1H, J = 1.93 Hz, J = 10.68 Hz, H_6); 4.05 (dd, 1H, J = 6.43 Hz, J = 10.68 Hz, H_6'); 3.52−3.43 (m, 2H, H_3−H_5); 3.21−3.09 (m, 4H, OCH_3, H_2); 2.98 (m, 1H, H_4); 2.42 (s, 3H, CH_3). $^{13}C\{^1H\}$ NMR (75 MHz, D_2O, 298 K): δ 145.5 (C_a); 132.9 (C_d); 130.8 (C_c); 128.2 (C_b); 100.3 (C_1); 73.6 (C_3); 72.2 (C_2); 70.9 (C_6); 70.3 (C_4); 70.0 (C_5); 55.1 (OCH_3); 21.7 (CH_3).

■ ASSOCIATED CONTENT

Ⓢ Supporting Information

NMR data, UV−vis spectra, water solubility of carbonate bases, mass spectra, and kinetic profiles. The Supporting Information is available free of charge on the ACS Publications website at DOI: 10.1021/acs.joc.5b00697.

■ AUTHOR INFORMATION

Corresponding Author

*E-mail: frederic.hapiot@univ-artois.fr.

Notes

The authors declare no competing financial interest.

■ ACKNOWLEDGMENTS

Roquette Frères (Lestrem, France) is gratefully acknowledged for generous gifts of cyclodextrins. We thank Dr. Nicolas Kania and D. Prevost for technical assistance.

■ REFERENCES

(1) Dodziuk, H. In *Cyclodextrins and Their Complexes: Chemistry, Analytical Methods, Applications*; Dodziuk, H., Ed.; Wiley-VCH: Weinheim, Germany, 2006.

(2) Arun, R.; Ashok Kumar, C. K.; Sravanthi, V. V. N. S. S. *Sci. Pharm.* **2008**, *76*, 567−598.

(3) Loftsson, T.; Duchêne, D. *Int. J. Pharm.* **2007**, *329*, 1−11.

(4) Jazkewitsch, O.; Ritter, H. *Macromolecules* **2011**, *44*, 375−382.

(5) Perry, C.; Hébraud, P.; Gernigon, V.; Brochon, C.; Lapp, A.; Lindner, P.; Schlatter, G. *Soft Matter* **2011**, *7*, 3502−3512.

(6) Harada, A.; Li, J.; Kamachi, M. *Nature* **1992**, *356*, 325−327.

(7) Peters, O.; Ritter, H. *Angew. Chem., Int. Ed.* **2013**, *52*, 1−6.

(8) Li, J. *Adv. Polym. Sci.* **2009**, *222*, 79−113.

(9) Wagner, B. D. In *Cyclodextrin Materials Photochemistry, Photophysics and Photobiology*; Douhal, A., Ed.; Elsevier: Amsterdam, 2006.

(10) Smaldone, R. A.; Forgan, R. S.; Furukawa, H.; Gassensmith, J. J.; Slawin, A. M. Z.; Yaghi, O. M.; Stoddart, J. F. *Angew. Chem., Int. Ed.* **2010**, *49*, 8630−8634.

(11) Woggon, W.-D.; Schlatter, A.; Wang, H. β-Cyclodextrin-linked Ru Complexes for Oxidations and Reductions. In *Advances in Inorganic Chemistry*; van Eldik, R., Ed.; Academic Press: The Netherlands, 2008; Vol. *60*, pp 31−58.

(12) Schlatter, A.; Woggon, W.-D. *Adv. Synth. Catal.* **2008**, *350*, 995−1000.

(13) Machut, C.; Patrigeon, J.; Tilloy, S.; Bricout, H.; Hapiot, F.; Monflier, E. *Angew. Chem., Int. Ed.* **2007**, *46*, 3040−3042.

(14) Kanagaraj, K.; Pitchumani, K. *Chem.—Eur. J.* **2013**, *19*, 14425−14431.

(15) Doyagüez, E. G.; Rodríguez-Hernández, J.; Corrales, G.; Fernández-Mayoralas, A.; Gallardo, A. *Macromolecules* **2012**, *45*, 7676−7683.

DOI: 10.1021/acs.joc.5b00697
J. Org. Chem. 2015, 80, 6259−6266

(16) Hapiot, F.; Bricout, H.; Menuel, S.; Tilloy, S.; Monflier, E. *Catal. Sci. Technol.* **2014**, *4*, 1899−1908.
(17) Breslow, R.; Dong, S. D. *Chem. Rev.* **1998**, *98*, 1997−2011.
(18) Bjerre, J.; Rousseau, C.; Marinescu, L.; Bols, M. *Appl. Microbiol. Biotechnol.* **2008**, *81*, 1−11.
(19) Furukawa, Y.; Ishiwata, T.; Sugikawa, K.; Kokado, K.; Sada, K. *Angew. Chem., Int. Ed.* **2012**, *51*, 10566−10569.
(20) Zerkoune, L.; Angelova, A.; Lesieur, S. *Nanomaterials* **2014**, *4*, 741−765.
(21) Tiwari, G.; Tiwari, R.; Rai, A. K. *J. Pharm. BioAllied Sci.* **2010**, *2*, 72−79.
(22) Otero-Espinar, F. J.; Torres-Labandeira, J. J.; Alvarez-Lorenzo, C.; Blanco-Méndez, J. *J. Drug Delivery Sci. Technol.* **2010**, *20*, 289−301.
(23) Rauf Khan, A.; Forgo, P.; Stine, K. J.; D'Souza, V. T. *Chem. Rev.* **1998**, *98*, 1977−1996.
(24) Fukudome, M.; Onizuka, T.; Kawamura, S.; Yuan, D.-Q.; Fujita, K. *Tetrahedron Lett.* **2007**, *48*, 6665−6668.
(25) Teranishi, K. *Tetrahedron* **2003**, *59*, 2519−2538.
(26) Tang, W.; Ng, S.-C. *Nat. Protoc.* **2008**, *3*, 691−697.
(27) Guieu, S.; Sollogoub, M. *Angew. Chem., Int. Ed.* **2008**, *47*, 7060−7063.
(28) Ghosh, R.; Zhang, P.; Wang, A.; Ling, C.-C. *Angew. Chem., Int. Ed.* **2012**, *51*, 1548−1552.
(29) Zaborova, E.; Guitet, M.; Prencipe, G.; Blériot, Y.; Ménand, M.; Sollogoub, M. *Angew. Chem., Int. Ed.* **2013**, *52*, 639−644.
(30) James, S. L.; Adams, C. J.; Bolm, C.; Braga, D.; Collier, P.; Friščić, T.; Grepioni, F.; Harris, K. D. M.; Hyett, G.; Jones, W.; Krebs, A.; Mack, J.; Maini, L.; Orpen, A. G.; Parkin, I. P.; Shearouse, W. C.; Steed, J. W.; Waddell, D. C. *Chem. Soc. Rev.* **2012**, *41*, 413−447.
(31) Ralphs, K.; Hardacre, C.; James, S. L. *Chem. Soc. Rev.* **2013**, *42*, 7701−7718.
(32) Šepelák, V.; Bégin-Colin, S.; Le Caër, G. *Dalton Trans.* **2012**, *41*, 11927−11948.
(33) Boldyreva, E. *Chem. Soc. Rev.* **2013**, *42*, 7719−7738.
(34) Perejón, A.; Murafa, N.; Sánchez-Jiménez, P. E.; Criado, J. M.; Subrt, J.; Diánez, M. J.; Pérez-Maqueda, L. A. *J. Mater. Chem. C* **2013**, *1*, 3551−3562.
(35) Huskić, I.; Halasz, I.; Friščić, T.; Vančik, H. *Green Chem.* **2012**, *14*, 1597−1600.
(36) Štrukil, V.; Bartolec, B.; Portada, T.; Đilović, I.; Halaszc, I.; Margetić, D. *Chem. Commun.* **2012**, *48*, 12100−12102.
(37) Stolle, A.; Szuppa, T.; Leonhardt, S. E. S.; Ondruschka, B. *Chem. Soc. Rev.* **2011**, *40*, 2317−2329.
(38) Choudhary, G.; Krishna Peddinti, R. *Green Chem.* **2011**, *13*, 276−282.
(39) Štrukil, V.; Igrc, M. D.; Fábián, L.; Eckert-Maksić, M.; Childs, S. L.; Reid, D. G.; Duer, M. J.; Halasz, I.; Mottillo, C.; Friščić, T. *Green Chem.* **2012**, *14*, 2462−2473.
(40) Konnert, L.; Gauliard, A.; Lamaty, F.; Martinez, J.; Colacino, E. *ACS Sustainable Chem. Eng.* **2013**, *1*, 1186−1191.
(41) Zhu, S.-E; Li, F.; Wang, G.-W. *Chem. Soc. Rev.* **2013**, *42*, 7535−7570.
(42) Wang, G.-W *Chem. Soc. Rev.* **2013**, *42*, 7668−7700.
(43) Liu, Z.; Fan, G.-P.; Wang, G.-W. *Chem. Commun.* **2012**, *48*, 11665−11667.
(44) Fan, G.-P.; Liu, Z.; Wang, G.-W. *Green Chem.* **2013**, *15*, 1659−1664.
(45) Štrukil, V.; Fábián, L.; Reid, D. G.; Duer, M. J.; Jackson, G. J.; Eckert-Maksić, M.; Friščić, T. *Chem. Commun.* **2010**, *46*, 9191−9193.
(46) Adams, C. J.; Kurawa, M. A.; Orpen, A. G. *Dalton Trans.* **2010**, *39*, 6974−6984.
(47) Içli, B.; Christinat, N.; Tönnemann, J.; Schüttler, C.; Scopelliti, R.; Severin, K. *J. Am. Chem. Soc.* **2009**, *131*, 3154−3155.
(48) Hsu, C.-C.; Chen, N.-C.; Lai, C.-C.; Liu, Y.-H.; Peng, S.-M.; Chiu, S.-H. *Angew. Chem., Int. Ed.* **2008**, *47*, 7475−7478.
(49) Carli, F. *Proc. Int. Symp. Controlled Release Bioact. Mater.* **1999**, *26*, 873−874.
(50) Kumar, V.; Taxak, N.; Jangir, R.; Bharatam, P. V.; R.Kartha, K. P. *J. Org. Chem.* **2014**, *79*, 3427−3439.
(51) Kumar, V.; Yadav, N.; Kartha, K. P. *Carbohydr. Res.* **2014**, *397*, 18−26.
(52) Rinaldi, L.; Binello, A.; Stolle, A.; Curini, M.; Cravotto, G. *Steroids* **2015**, *98*, 58−62.
(53) Braga, D.; Grepioni, F. *Angew. Chem., Int. Ed.* **2004**, *43*, 4002−4011 and references therein..
(54) Lin, H.-L.; Lin, S.-Y.; Lin, C.-C.; Hsu, C.-H.; Wu, T.-K.; Huang, Y.-T. *Carbohydr. Polym.* **2012**, *87*, 512−517.
(55) Martina, K.; Trotta, F.; Robaldo, B.; Belliardi, N.; Jicsinszky, L.; Cravotto, G. *Tetrahedron Lett.* **2007**, *48*, 9185−9189.
(56) Tan, T.; Ng, S.-c.; Wang, Y.; Xiao, Y. *Protoc. Exch.* **2011**, DOI: 10.1038/protex.2011.214.
(57) Law, H.; Benito, J. M.; Garcıa Fernandez, J. M.; Jicsinszky, L.; Crouzy, S.; Defaye, J. *J. Phys. Chem. B* **2011**, *115*, 7524−7532.
(58) Ueno, A.; Breslow, R. *Tetrahedron Lett.* **1982**, *23*, 3451−3454.
(59) Rong, D.; D'Souza, V. T. *Tetrahedron Lett.* **1990**, *31*, 4275−4278.
(60) Teranishi, K.; Watanabe, K.; Hisamatsu, M.; Yamada, T. *J. Carbohydr. Res.* **1998**, *17*, 489−494.
(61) Teranishi, K.; Tanabe, S.; Hisamatsu, M.; Yamada, T. *Biosci. Biotechnol. Biochem.* **1998**, *62*, 1249−1252.
(62) Fukudome, M.; Oiwane, K.; Mori, T.; Yuan, D.-Q.; Fujita, K. *Tetrahedron Lett.* **2004**, *45*, 3383−3386.
(63) Yu, H.; Teramoto, A.; Fukudome, M.; Xie, R.-G.; Yuan, D.-Q.; Fujita, K. *Tetrahedron Lett.* **2006**, *47*, 8837−8840.
(64) Wang, Z.-Z.; He, G.-Y.; Lu, R.-H. *Monatsh. Chem.* **2008**, *139*, 1109−1111.
(65) Wang, Z.-Z.; Fu, X.-Y.; Dai, G.-D.; Quan, H.-F. *Monatsh. Chem.* **2011**, *142*, 317−319.
(66) Law, H.; Baussanne, I.; Garcia Fernandez, J. M.; Defaye, J. *Carbohydr. Res.* **2003**, *338*, 451−453.
(67) Pregel, M. J.; Buncel, E. *Can. J. Chem.* **1991**, *69*, 130−137.
(68) van Dienst, E.; Snellink, B. H. M.; von Piekartz, I.; Gansey, M. H. B. G.; Venema, F.; Feiters, M. C.; Nolte, R. J. M.; Engbersen, J. F. J.; Reinhoudt, D. N. *J. Org. Chem.* **1995**, *60*, 6537−6545.
(69) Pessine, F. B. T.; Calderini, A.; Alexandrino G. L. Review: Cyclodextrin Inclusion Complexes Probed by NMR Techniques, Magnetic Resonance Spectroscopy. Kim, D.-H., Ed.; ISBN: 978-953-51-0065-2, InTech; Available from: http://www.intechopen.com/books/magneticresonance-spectroscopy/review-study-of-inclusion-complexes-with-cyclodextrins-by-mrs; 2012.
(70) Saalwächter, K. *Macromol. Rapid Commun.* **2002**, *23*, 286−291.
(71) Saalwächter, K.; Lange, F.; Matyjaszewski, K.; Huang, C.-F.; Graf, R. *J. Magn. Reson.* **2011**, *212*, 204−215.
(72) Sivakumar, K.; Hemalatha, G.; Parameswari, M.; Stalin, T. *Phys. Chem. Liq.* **2013**, *51*, 567−585.
(73) Betzel, C.; Saenger, W.; Hingerty, B. E.; Brown, G. M. *J. Am. Chem. Soc.* **1984**, *106*, 7545−7557.
(74) Gaidamauskas, E.; Norkus, E.; Butkus, E.; Crans, D. C.; Grincienė, G. *Carbohydr. Res.* **2009**, *344*, 250−254.
(75) Luty, T.; Eckhardt, C. J. *J. Am. Chem. Soc.* **1995**, *117*, 2441−2452.
(76) Ohashi, Y. *Acc. Chem. Res.* **1988**, *21*, 268−274.
(77) Coville, N. J.; Levendis, D. C. *Eur. J. Inorg. Chem.* **2002**, 3067−3078.
(78) Biedermann, F.; Nau, W. M.; Schneider, H.-J. *Angew. Chem., Int. Ed.* **2014**, *53*, 11158−11171.
(79) Friščić, T. *Chem. Soc. Rev.* **2012**, *41*, 3493−3510.
(80) Fung, B. M.; Khitrin, A. K.; Ermolaev, K. *J. Magn. Reson.* **2000**, *142*, 97−101.
(81) Carravetta, M.; Eden, M.; Zhao, X.; Brinkmann, A.; Levitt, M. H. *Chem. Phys. Lett.* **2000**, *321*, 205−215.
(82) Schneider, H.-J.; Hacket, F.; Rüdiger, V. *Chem. Rev.* **1998**, *98*, 1755−1785.
(83) Van der Eijk, J. M.; Nolte, R. J. M.; Zwikker, J. W. *J. Org. Chem.* **1980**, *45*, 547−548.

DOI: 10.1021/acs.joc.5b00697
J. Org. Chem. 2015, 80, 6259−6266